Real-valued Delayless Subband Affine Projection Algorithm for Acoustic Echo Cancellation

Hesu Huang and Chris Kyriakakis
Immersive Audio Laboratory
Integrated Media Systems Center
University of Southern California, Los Angeles, CA 90089

***Abstract* - Acoustic Echo Cancellation (AEC) often involves adaptive filters with large numbers of taps, which results in poor performance in real-time applications. The utilization of Delayless Subband Adaptive Filter (DSAF) helps reduce computations and improve the overall performance. However, conventional oversampled subband adaptive filters mainly use DFT or GDFT based analysis/synthesis filter banks and generate "complex-valued" subband signals. This is particularly inefficient when applying the Affine Projection Algorithm (APA), a popular adaptive algorithm for AEC problem, to each subband. For APA implementation, real-valued signals show higher efficiency than complex signals. In this paper, we present a real-valued delayless subband APA and study both its computational complexity and performance on AEC problems. Compared to the complex valued approach, our method achieves a better performance with lower computational cost.**

I. Introduction

Affine Projection Algorithm (APA) is widely used in Acoustic Echo Cancellation (AEC) applications due to its improved performance compared to LMS algorithms and lower computational complexity than RLS algorithms. However, a real acoustic echo canceller often involves adaptive filters with large numbers of taps, which results in heavy computational burden and slow convergence speed. The large dynamic range of audio signal further deteriorates its performance. Hence, APA is often combined with Subband Adaptive Filters (SAF) to save computational cost and accelerate convergence speed [1].

A problem with SAF is that a substantial delay is introduced into the signal path by analysis/synthesis filter banks. This is particularly undesirable in real-time AEC applications. Morgan and Thi [2] proposed Delayless Subband Adaptive Filtering (DSAF) to overcome this problem. However, conventional DSAF usually uses DFT or GDFT based analysis/synthesis filter banks [3] [3], in which the generated subband signals are "complex-valued". This introduces additional complexity when combining the APA algorithm with the DSAF approach in AEC, as implementing APA with complex-valued signals is more complicated than with real-valued signals.

In this paper, we present a real-valued oversampled delayless subband APA based on GDFT analysis filter banks. In particular, we generate the real-valued subband signals by applying Single Side Band (SSB) modulation [3] on the complex GDFT filter banks. The real-valued signals simplify the implementation of APA on each subband and reduce the computational complexity of the overall AEC systems. Furthermore, the use of delayless SAF eliminates the inherent delay existed in SAF systems. As such, our system is more efficient and well-suited for real-time AEC applications.

This paper is organized as follows: in Section II, we describe the real-valued DSAF structure and the implementation of APA algorithm. Section III presents the complexity analysis of our proposed method and compares it with that of complex-valued DSAF using APA algorithm. Finally, we present experimental results to demonstrate the efficiency of our method in Section IV.

II. System architecture

A. Delayless SAF Structure

Fig.1 shows the overall system structure of a real-valued Delayless Subband Acoustic Echo Canceller based on APA.

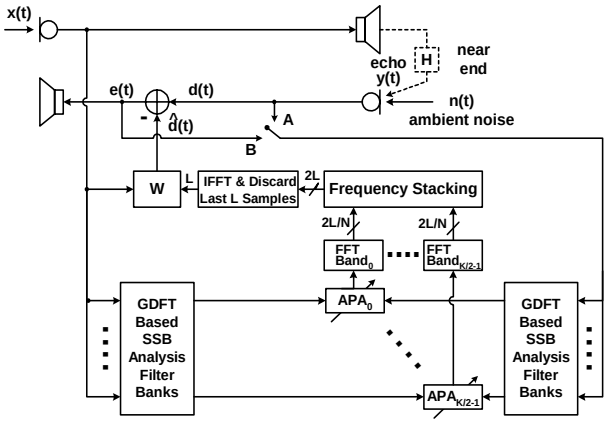

Fig.1: Real-valued Delayless Subband APA AEC system
Position A: Open-Loop; Position B: Closed-Loop

In contrast to the conventional SAF structure which requires both analysis and synthesis filters, Delayless SAF avoids using synthesis filter banks by employing a weight transformation technique to transform the subband filter

Report Documentation Page

Form Approved
OMB No. 0704-0188

1. REPORT DATE	2. REPORT TYPE	3. DATES COVERED
2006		**00-00-2006 to 00-00-2006**

4. TITLE AND SUBTITLE	5a. CONTRACT NUMBER
Real-valued Delayless Subband Affine Projection Algorithm for Acoustic Echo Cancellation	5b. GRANT NUMBER
	5c. PROGRAM ELEMENT NUMBER
6. AUTHOR(S)	5d. PROJECT NUMBER
	5e. TASK NUMBER
	5f. WORK UNIT NUMBER
7. PERFORMING ORGANIZATION NAME(S) AND ADDRESS(ES) **University of Southern California,Immersive Audio Laboratory,Integrated Media Systems Center,Los Angeles,CA,90089**	8. PERFORMING ORGANIZATION REPORT NUMBER
9. SPONSORING/MONITORING AGENCY NAME(S) AND ADDRESS(ES)	10. SPONSOR/MONITOR'S ACRONYM(S)
	11. SPONSOR/MONITOR'S REPORT NUMBER(S)

12. DISTRIBUTION/AVAILABILITY STATEMENT
Approved for public release; distribution unlimited

13. SUPPLEMENTARY NOTES

14. ABSTRACT

15. SUBJECT TERMS

16. SECURITY CLASSIFICATION OF:			17. LIMITATION OF ABSTRACT	18. NUMBER OF PAGES	19a. NAME OF RESPONSIBLE PERSON
a. REPORT **unclassified**	b. ABSTRACT **unclassified**	c. THIS PAGE **unclassified**		**4**	

weights into fullband filter weights. Thus the transmission delay can be eliminated due to the fact that the signal for canceling the desired signal is computed by the fullband filter. The Delayless SAF can be divided into two categories: open-loop type (Position *A* in Fig.1), and closed-loop type (Position *B* in Fig.1). Generally speaking, open-loop scheme will give less suppression since the algorithm is working blindly with respect to the real error signal. In this paper, both of these two schemes are implemented and studied.

B. Single-Sideband (SSB) Analysis Filter Banks

Since the implementation of APA is easier with non-complex arithmetic, real-valued subband signals are preferred on each subband. To obtain real-valued oversampled filter banks, we can use either non-uniform filter banks [4] or SSB modulated filter banks [3]. The former scheme typically needs to deal with different subsampling rates. Therefore, we focus on SSB filter banks implementation here.

It is known that SSB filter banks can be obtained by postprocessing complex-valued Generalized DFT (GDFT) filter banks properly [3]. Below we first describe GDFT briefly. The GDFT transform pair is defined as:

$$Y_k^{GDFT} = \sum_{n=0}^{K-1} y(n) W_K^{-(k+k_0)(n+n_0)}, \quad k = 0,1,....,K-1$$
$$y(n) = \frac{1}{K}\sum_{k=0}^{K-1} Y_k^{GDFT} W_K^{(k+k_0)(n+n_0)}, \; n = 0,1,....,K-1 \qquad (1)$$

where K is the number of subbands, and $W_K = e^{j(2\pi/K)}$. The analysis filter bank equation based on GDFT is then:

$$X_k^{GDFT}(m) = \sum_{n=-\infty}^{\infty} h(mN-n)x(n)W_K^{-(k+k_0)(n+n_0)} \qquad (2)$$
$$k = 0,1,....,K-1$$

where *h(n)* is the lowpass prototype filter for analysis filter banks, N is the decimation factor, and L_p is the length of prototype filter *h(n)*. In this paper, we only discuss the case for $k_0=1/2$, $n_0=-(L_p-1)/2$. Therefore, SSB signal $X_k^{SSB}(m)$ can be expressed in terms of GDFT signal as:

$$X_k^{SSB}(m) = \mathrm{Re}[X_k^{GDFT}(m) e^{j\omega_\Delta mN/2}] \qquad (3)$$

where $\omega_\Delta = \pi/N$ is the bandwidth of the prototype *h(n)*. Obviously, the decimation factor for real-valued SSB filter banks is $N = \pi/\omega_\Delta$. Compared to the decimation factor for a complex-valued GDFT filter banks, $N_c = 2\pi/\omega_\Delta$, we can conclude that N is approximately half of N_c, i.e. $N \approx N_c/2$, because of the real operation in SSB.

Because the prototype filter *h(n)* design is identical to the design for complex-valued GDFT filter banks, we used the fast converging iterative least squares method provided by Weiss [5] to design *h(n)*. This method has the advantages of sufficiently suppressing the aliasing.

The implementation of SSB filter banks for k_{th} channel is shown in Fig.2(a). In this way, several efficient methods to realize GDFT filter banks can be directly applied to the realization of SSB filter banks. In this paper, we employ the efficient polyphase implementation of the GDFT filter banks proposed by Weiss in [5], which is suitable for any integer decimation factor $N < K/2$.

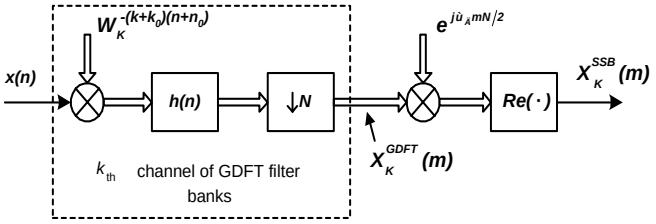

Fig.2(a): Block diagram of SSB filter bank analyzer based on GDFT filter bank for the k_{th} channel.

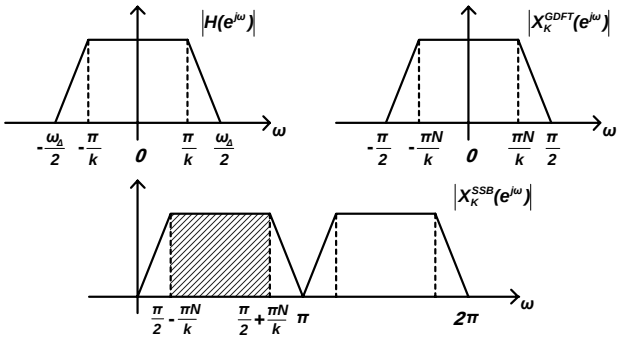

Fig.2(b): Spectrum of Prototype Filter, k_{th} channel of GDFT Analysis Filter Bank and SSB Analysis Filter Bank

C. Weight Transform

Originally, Morgan suggested a FFT-stacking transform for complex-valued DSAF [2]. But when it is interpreted as a synthesis filter bank, the nulls in the passbands of the synthesis filters deteriorate the performance. A FFT-2 weight transform presented in [6] showed a significant improvement in performance. In this paper, we design a new stacking rule based on the similar FFT-2 weight transform.

In Fig.2(b), observe that all real-valued subband signals are modulated to baseband. This enables us to obtain the relations among fullband and real-valued subband signals. The following equation shows the frequency stacking rules:

$$W(l) = \begin{cases} W_{[\frac{Kl}{2L}]}((l)_{\frac{2L}{K}} + \frac{L}{2N} - \frac{L}{K}) & l \in [0, L) \\ 0 & l = L \\ W(2L-l)^* & l \in (L, 2L) \end{cases} \qquad (4)$$

where L is the length of the fullband filter, and is assumed to be dividable by the LCM of K and $2N$. $W(l)$ and $W_k(l)$ stand for the l_{th} FFT coefficients of fullband filter and the k_{th} subband filter respectively. Here $[a]$ denotes the closest integer smaller than a, and $(a)_b$ means 'a modulus b'.

III. Computational complexity analysis

Our analysis is based on the conclusion made in Section 2.2 that $N \approx N_c/2$ holds approximately. According to [2], the computational load required for a DSAF, both with real-valued signals and with complex-valued signals, can be divided into four components: subband filtering, subband adaptive filtering (APA in this paper), weight transformation, and the signal path convolution with fullband filter W. The computation complexity of the last two components for real-valued DSAF is same as that for complex-valued DSAF, so we focus on the analysis of first two parts.

SUBBAND FILTERING: Let R_1^c denote the computational requirement of complex-valued subband decomposition and R_1^r that of real-valued delayless subband decomposition. For a GDFT analysis filter bank, if polyphase FFT implementation is used, we need

$$R_1^c \approx (L_p + K\log_2 K + 4K)/N_c \tag{5}$$

real multiplications per input sample [2], where L_p represents the length of prototype filter *h(n)*. For the corresponding real-valued SSB filter banks, SSB modulation requires additional *K/N* multiplications per sample. Since $N \approx N_c/2$, we conclude that real-valued SSB filter banks usually require twice computations as GDFT filter banks, i.e. $R_1^r \approx 2\,R_1^c$. However, compared with the computational savings in the second step (see analysis below), this overhead is small and ignorable.

SUBBAND ADAPTIVE FILTERING: When Fast APA is used and the subband signals are real-valued, the computational requirement in this step is *2M+20P* real multiplications per sample [7]. Here *M* is the adaptive filter order and *P* is the projection order. As each complex multiplication requires four real multiplications, it is easy to obtain the computational requirement for real-valued DSAF and complex-valued DSAF.

$$R_2^r = \frac{1}{N}(2\frac{L}{N} + 20P) * \frac{K}{2} \tag{6}$$

$$R_2^c = \frac{4}{N_c}(2\frac{L}{N_c} + 20P) * \frac{K}{2} \tag{7}$$

Replacing N_c with *2N*, we get the ratio between them:

$$\frac{R_2^c}{R_2^r} = \frac{(2L/N + 40P) * K/2}{(2L/N + 20P) * K/2} \tag{8}$$

In AEC applications, projection order *P* is often set to a value like 8 or 16, which, after multiplied by 20 or 40, is much larger than *2L/N*. In this case, *P* becomes the dominant factor in deciding R_2. Approximately, we have $R_2^c \approx 2\,R_2^r$.

Note that from the above analysis, the computational load for subband APA can be highly independent of its adaptive filter length when *P* is large. In summary, the real-valued delayless subband APA implementation requires less computational power and is more efficient.

IV. Computer simulations

The impulse response to model the echo path in our simulations is a small room impulse response, truncated with 1024 taps. Consequently, the number of the fullband filter taps *L* is chosen as 1024. The sampling frequency is 22050 Hz in the fullband. The adaptations are performed in *K=128* subbands with a decimation factor of *N=32* for real-valued DSAF and a decimation factor of N_c*=64* for complex-valued DSAF. In addition, we assumed that there are no near-end speech/music signals. Instead, an ambient noise *n(n)* with a fixed SNR of 30dB is added into the near-end microphone (see Fig.1). The measure of Echo Return Loss Enhancement (ERLE) curves are presented in the simulation results. ERLE is defined as

$$ERLE = 10\log_{10}(\frac{E[y(n)^2]}{E[e(n)^2]}) \tag{9}$$

A. ERLE Convergence Plots for White Noise Input x(n)

Fig.3 shows the ERLE convergence of our proposed real-valued delayless subband APA with white noise input. For the open-loop scheme (Fig.3(a)), the results for both complex-valued delayless subband RLS algorithm and complex-valued delayless subband APA are depicted for comparison purpose, while complex-valued delayless subband NLMS and complex-valued delayless subband APA were compared in closed-loop scheme (Fig.3(b)). Obviously, compared to complex-valued delayless subband APA, our proposed real-valued delayless subband APA achieves better performance in terms of both ERLE convergence speed and ERLE level. The increase in projection order *P* from 2nd to 4th demonstrates a faster ERLE convergence rate and closer performance to RLS algorithm. Furthermore, the closed-loop scheme can achieve a higher echo suppression level once it converges.

B. ERLE Convergence Plots for Real Music Input

Fig.4 shows the performance of our proposed real-valued delayless subband APA for real music input. Since the performance of our proposed real-valued delayless subband APA is very close to its complex-valued counterpart for real music input, we only compare it to the conventional complex-valued delayless subband RLS for open-loop scheme (Fig.4(a)) and delayless subband NLMS for closed-loop scheme (Fig.4(b)) respectively. Similar performance improvements as in the case with white noise are observed. However, the performance improvement caused by increasing *P* is not so significant.

V. Conclusions

In this paper, we proposed a real-valued delayless subband affine projection algorithm (APA) and applied it to acoustic echo cancellation applications. The system imple-

mentation details were presented and the computation complexity was analyzed. The simulation results show that its performance, in terms of ERLE level and convergence speed, is better than that of conventional complex-valued DSAF. In addition, the computational complexity of our proposed approach is in most cases less than its complex-valued counterpart.

ACKNOWLEDGEMENTS

Research presented this paper was funded in part by the Integrated Media Systems Center, a National Science Foundation Engineering Research Center, Cooperative Agreement No. EEC-9529152 and in part by the Department of the Army under contract number DAAD 19-99-D-0046. Any opinions, findings and conclusions or recommendations expressed in this material are those of the authors and do not necessarily reflect those of the National Science Foundation and the Department of the Army.

REFERENCES

[1] Nakagawa, A., Haneda, Y., and Makino, S. "Subband acoustic echo canceller using two different analysis filters and 8th order projection algorithm," *Proc. Intern. Workshop On Acoustic Echo and Noise Control*, pp. 140-143, Imperial College, London, 1997.

[2] Morgan, D.R. and Thi, J.C. "A delayless subband adaptive filter architecture," *IEEE Trans. Signal Processing*, vol. 43, No. 8, pp. 1819-1830, 1995.

[3] Crochiere, R.E., and Rabiner, L.R. *Multirate digital signal processing*, Prentice-Hall,Inc., Englewood Cliffs, New Jersey, 1983.

[4] Harteneck, M., Weiss, S. and Stewart, R W. "Design of near perfect reconstruction oversampled filter banks for subband adaptive filters ", *IEEE Trans. Circuits and Systems*, vol. 46, pp. 1081-10851, 1999.

[5] Weiss, S and Harteneck, M and Stewart, R W. "On implementation and design of filter banks for subband adaptive systems", *Proc. IEEE Workshop on Signal Processing Systems*, pp. 172-181, 1998.

[6] Huo, J., Nordholm, S. and Zang, Z. "New weight transform schemes for delayless subband adaptive filtering ", *Global Telecommunications Conference, 2001. GLOBECOM '01.* IEEE, vol. 1, pp. 197-201, 2001.

[7] Gay, S.L. and Tavathia, S. "The fast affine projection algorithm," *Proc. International Conf. Acoustics, Speech, and Signal Processing*, vol. 5, pp.3023-3026, 1995.

[8] Vaidyanathan, P., *Multirate systems and filter banks*, Prentice Hall, Inc., 1993

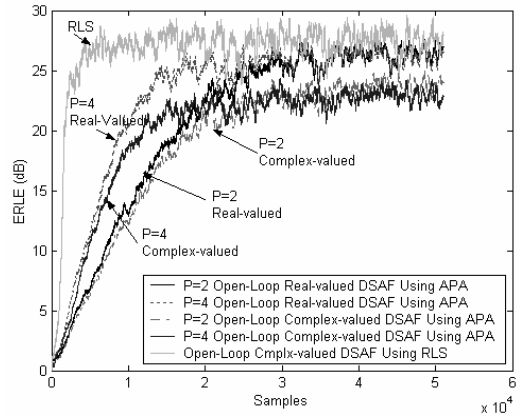

Fig.3(a): *ERLE Convergence for White Noise Input using Open-Loop Configuration*: Our proposed Real-Valued Delayless Subband APA shows a closer performance to Conventional Complex-Valued Delayless Subband RLS than Complex-valued case.

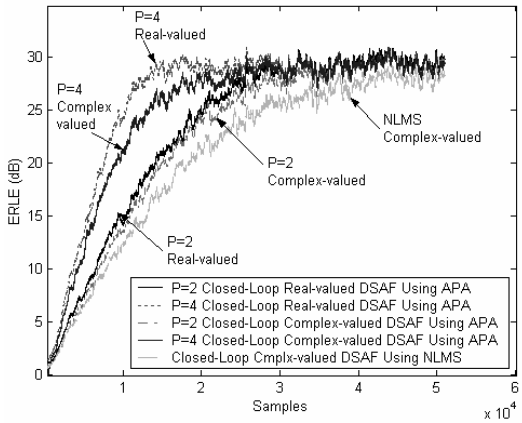

Fig.3(b): *ERLE Convergence for White Noise Input using Closed-Loop Configuration*: Our proposed Real-Valued Delayless Subband APA shows a better performance than Conventional Complex-valued Delayless Subband NLMS/APA.

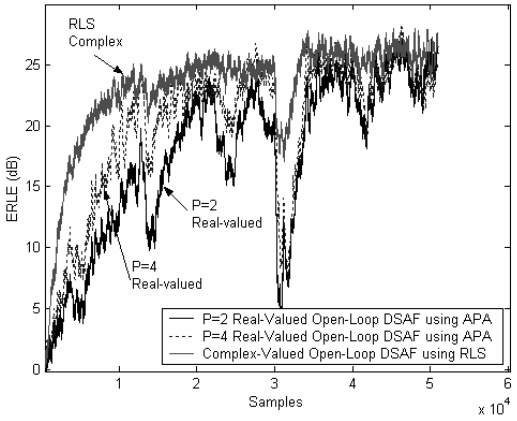

Fig.4(a): *ERLE Convergence for Real Music Input using Open-Loop Configuration*: Our proposed Real-Valued Delayless Subband APA shows a closer performance to Conventional Complex-Valued Delayless Subband RLS when *P* is increased.

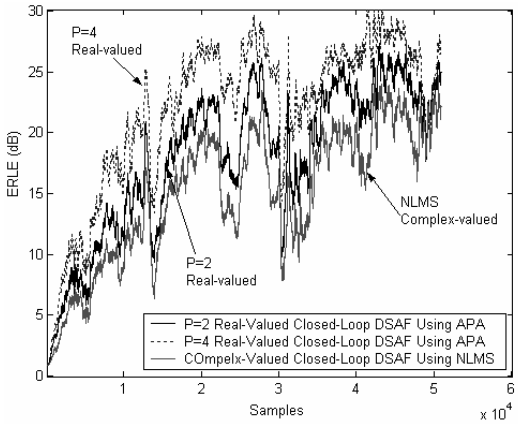

Fig.4(b): *ERLE Convergence for Real Music Input using Closed-Loop Configuration*: Our proposed Real-Valued Delayless Subband APA shows a better performance than Conventional Complex-Valued Delayless Subband NLMS for real music input.